A Vision-based Shared Autonomy Framework for Deformable Linear Objects Manipulation

A Vision-based Shared Autonomy Framework for Deformable Linear Objects Manipulation

Davide Chiaravalli, Alessio Caporali, Anna Friz, Roberto Meattini and Gianluca Palli

***Abstract*—The manipulation of Deformable Linear Objects (DLOs) is a critical process in which the introduction of automation and autonomous systems is still marginal. In this paper, a novel teleoperation framework is proposed in which an intuitive manipulation of DLOs is achieved by means of visual aid. The proposed system could be deployed for manipulating DLOs in hazardous scenarios or for simplifying robot teaching tasks by allowing a faster demonstration time. Experiments are performed involving several subjects and their feedback is collected by means of a survey. The results show that the proposed teleoperation framework simplifies DLOs manipulation and reduces the task completion time by 20% on average.**

***Index Terms*—Shared Autonomy, Teleoperation, Deformable Linear Objects**

I. Introduction

In the last decade, the introduction of automation in industrial processes and plants and the improvement of vision systems have pushed researchers toward new directions, aiming at developing advanced interaction capabilities and flexibility in the control processes. Among them, great focus was given to the modeling and manipulation of Deformable Linear Objects (DLOs) because of their key role in many industrial scenarios that cross several application fields such as automotive, domotic, or healthcare. To this purpose, several research projects have been promoted with the objective of further increasing the technological knowledge of these systems. The manipulation of a DLO is performed by tracking the objects either exploiting a mechanical deformation model [1] or continuously estimating its shape through a dedicated vision system [2]. Most applications directly involve continuous interaction between the manipulator and the DLO [3] with the purpose of imposing a certain shape [4] or successfully performing insertion tasks [2]. Given the complexity of the problem, several research studies have addressed DLO manipulation with a task-oriented strategy by either designing specific tools [5] or by directly defining separate modules to handle the different operations required [6]. Nonetheless, they lack the flexibility to allow task generalization in different scenarios. To this purpose, teleoperation still plays a central role for its capability to merge together the intuivity and flexibility to changes of a human operator, and the reactiveness and personalization of a robotic autonomous system. Moreover, it results as an effective solution in kinesthetic teaching frameworks where the robotic system is trained by directly transferring the human knowledge of the task [7].

In this work, we present a novel teleoperation framework able to allow intuitive manipulation of DLOs by means of an industrial robotic manipulator equipped with a vision system for DLO detection. The system aims to pose as an effective solution both for hazardous scenarios where human intervention is still required or for the definition of large datasets for robotic teaching. The paper is organized as follows: Sec. II provides an overview of the literature developed concerning both teleoperation and DLOs perception; Sec. III describes the system presenting the DLO detector and the teleoperation framework; Sec. IV shows the experimental process with a discussion of the results obtained; Sec. V draws the conclusions.

II. Related Works

A. Deformable Linear Objects Perception

The perception of DLOs has been commonly achieved by means of 2D cameras or tactile sensors. Indeed, the application of 3D cameras is usually constrained to specific scenarios and accomplished by means of high-end devices which are capable of sub-millimeter accuracy [8]. On the contrary, 2D cameras are vastly employed for detecting and segmenting DLOs. The common setups utilize simple color thresholding and background removal approaches [9]–[11] to achieve the perception of the DLO. Alternatively, deep learning-based methods, e.g. [12]–[14], have emerged to handle complex scenarios and backgrounds not tractable with simple approaches. Among the deep learning methods, *FASTDLO* [14] is currently the state-of-the-art method for the instance segmentation of DLOs, achieving processing speeds of above 20 FPS compared to the few FPS of *Ariadne+*, and employing a skeleton-based approach. These learning methods require the utilization of a dataset to optimize their model. In the literature, an approach for generating a dataset employing a chroma-key method is investigated in [15], which dataset is used in *Ariadne+* [13]. Recently, an approach investigating the utilization of a dataset composed of a mixture of synthetic and real images is proposed in [16].

B. Teleoperation

A teleoperation system allows a human operator to control a remote manipulator through a haptic system by recording the motion performed in a local workspace and replicating it in the remote environment. The replicated behavior is commonly

Davide Chiaravalli, Alessio Caporali, Anna Friz, Roberto Meattini and Gianluca Palli are with DEI - Department of Electrical, Electronic and Information Engineering, University of Bologna, Viale Risorgimento 2, 40136 Bologna, Italy.

This work was supported by the European Commission's Horizon 2020 Framework Programme with the project REMODEL - Robotic technologies for the manipulation of complex deformable linear objects - under grant agreement No 870133.

Corresponding author: *davide.chiaravalli2@unibo.it*

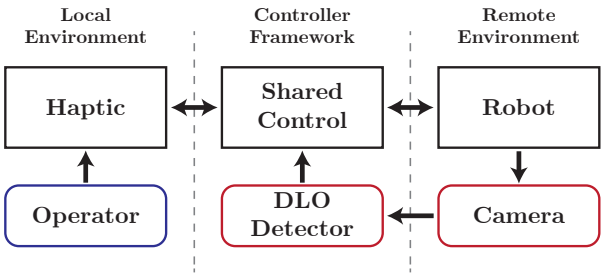

Fig. 1: Teleoperation framework.

driven by a predefined mapping function between the local and remote workspace. Such mapping plays a crucial role in the definition of the system performances and imposes a direct relation between the position or the velocities of the devices [17]. Despite their simplicity, these mappings usually produce low performances when dealing with workspaces of different dimensions. Therefore hybrid mappings exploiting different paradigms according to the sub-task executed or the environment conditions are usually preferred [18]. An interesting solution is given by edge drifting techniques [19], [20], that allow the local workspace to "drift" around the remote environment so that precise manipulation can be performed regardless of the workspace dimensions. Additional improvements are obtained when exploiting shared control strategies, where the system cooperates with the operator to produce a more intuitive control [21] with the aim of reducing the overall mental workload [22]. Recent works focused on simplifying the interaction with the environment by improving the precise interaction or grasping of the objects by exploiting the additional information provided through a vision system. In [23] the camera system is exploited to perceive the user intention and a shared control framework is exploited to guide the motion for the grasp. Similarly in [24] a guided system allows the operator to focus on the fine manipulation whereas the autonomous system handles the primitive motions toward the target. Nonetheless these solutions are specifically influenced by the task and require knowledge of the environment. Other solutions exploit the concept of virtual fixtures, force surfaces generated on the haptic device to improve the operator's perception of the environment to feel the presence of obstacles [25] or guide the user for the interaction [26]. Inspired by these works we propose a novel teleoperation system combining a vision system for cable localization and tracking and a shared control architecture for simplified grasping and manipulation. Moreover, we exploit virtual fixtures to guide the operator through the task and allow a clear perception of the cable shape. The proposed framework aims at simplifying DLO manipulation tasks in different environments since the only focus is the cable grasping and no preconception on the environment or task to be executed is considered.

III. System Description

In the following, a novel teleoperation framework for intuitive DLO manipulation is presented. The system, see Fig. 1, records the operator's motions through the haptic platform and replicates them in the remote environment. An RGB camera mounted on the end-effector of the remote manipulator allows for on-site quick reconstruction of the cable shape on operator demand as described in Sec. III-A. Then the DLO characterization produced is exploited to enhance the picking operation and successfully manipulate the environment to perform the required task. A clear description of the teleoperation system and the shared control framework is proposed in Sec. III-B.

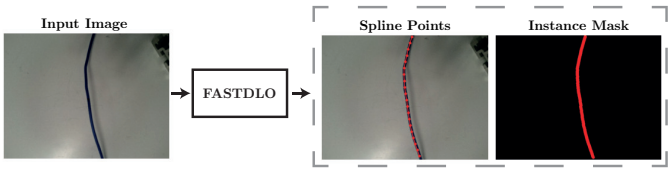

Fig. 2: DLO perception diagram with the spline of the detected DLO evaluated at $n = 20$ points.

A. DLOs Perception and Modeling

The perception of the DLO is achieved by employing the algorithm named *FASTDLO* [14]. The approach takes as input a 2D RGB image of the scene and provides as output the individual DLO instances composing it. In particular, the output of *FASTDLO* is twofold: 1) a colored mask where each DLO is densely labeled pixel-wise with a unique color identifying its ID; 2) a set of 2D splines in pixels coordinates where each spline describes a DLO instance. Concerning the latter, a generic DLO shape is represented in the image space by a 3rd-order spline basis as a function of a free coordinate u representing the position along the cable starting from an endpoint ($u = 0$) to the opposite end ($u = L$) being L the length of the DLO. That is:

$$q(u) = \sum_{i=1}^{n} b_i(u) q_i$$

where $q(u) = [p_x(u) \;\; p_y(u)]^T$ is the vector of pixel coordinates of each point along the DLO, $b_i(u)$ is the i-th elements of the spline polynomial basis used to represent the DLO shape and q_i are n properly selected coefficients, usually called *control points*, used to interpolate the DLO shape through the $b_i(u)$ function basis. An example of the output generated by *FASTDLO* is provided in Fig. 2.

Afterward, the spline is evaluated in a number n of points. Each of the obtained points is projected in the 3D cartesian space as $\vec{v} = {}^{c}T_r A \vec{p}$, where $\vec{v} = [x, y, z, 1]^T$ is the vector associated to the 3D point in the robot base frame, A is the intrinsic camera matrix obtained via camera calibration, ${}^{r}T_c$ is the transformation from camera to robot, and $\vec{p} = [p'_x, p'_y, w]^T$ where w is the scaling factor and $[wp'_x, wp'_y]^T$ the input pixel coordinates.

B. Teleoperation

The teleoperation framework aims at simplifying the DLO manipulation task by providing an intuitive interface to successfully perform DLO picking operations. The system alternates between two main control modes: *free teleoperation* and

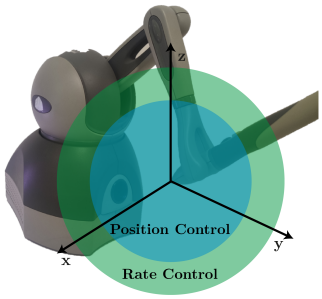

Fig. 3: 3DSystems Geomagic Touch haptic device

cable targeting modes.

In *free teleoperation mode* the remote manipulator's behavior is directly controlled through the operator's motions. The operator is able to freely move the robot in different workspace areas and interact with the environment.

In *cable targeting mode* the system performs a scan of the environment to search for existing cables and docks the robot to the most likely target (nearest DLO detected). By exploiting the points of the spline detected, the remote manipulator is then forced to move along the cable main dimension only, simplifying the grasping operation and guaranteeing finer control over the choice of the grasping point.

The operator during the task can freely switch between the two control modes by pressing a specific button on the stylus of the haptic device. This choice allows one to perform different tasks in the remote environment and exploit the cable targeting capabilities only when a cable grasp operation is required. In the following description, the reference frames of the haptic device and the remote manipulator O_h and O_r are considered for simplicity of notation to have the same axis orientation. A rotation ${}^{r}R_h \in \mathbb{R}^{3\times3}$ describing the haptic reference frame orientation O_h in the manipulator one O_r should be always applied in the general case for all the control mapping functions.

1) Free Teleoperation Mode: In this control mode, the operator fully controls the remote manipulator motion. An edge drifting mapping technique is employed to efficiently map the whole task environment: given the haptic stylus and the robot end-effector positions $P_h(t) \in \mathbb{R}^3$ and $P_r(t) \in \mathbb{R}^3$ respectively, a virtual spherical region or radius r_h centered in the zero coordinate of the haptic workspace is defined as shown in Fig. 3. Inside the spherical region a position control mapping is applied:

$$P_r(t) = K(P_h(t)) + D_{hr} \tag{1}$$

where $K \in \mathbb{R}^3$ is the scale factor that specifies the precision imposed by the mapping and $D_{hr} \in \mathbb{R}^3$ the initial mapping position bias from eq. 1 at time $t = 0$

$$D_{hr} = P_r(0) - K(P_h(0)) \tag{2}$$

In this area, the remote manipulator exactly replicates the scaled motion of the operator in the local workspace. Outside the spherical region, a rate control mapping is applied. The velocity of the manipulator $V_h(t) \in \mathbb{R}^3$ is controlled proportionally to the distance from the sphere:

$$\dot{P}_r(t) = K_v(P_h(t) - L_h(t)) \tag{3}$$

where $L_h(t) = r_h(P_h/\|P_h\|)$ is the intersection point of the position vector P_h with the spherical region and $K_v = V_{max}/(r_{max} - r_h)$ is the velocity gain designed to map the whole velocity range V_{max} of the manipulator.

The maximum radius r_{max} for the rate control region is defined as the radius of the largest sphere described inside the haptic workspace. An elastic force feedback is produced when moving in the rate control region to provide the operator with a clear perception of the commanded velocity. The force $F_h(t) \in \mathbb{R}^3$ is generated proportionally to the distance from the position control area:

$$F_h(t) = -K_f(P_h(t) - L_h(t)) \tag{4}$$

with $K_f(t) \in \mathbb{R}^3$ the feedback gain. Moreover, the feedback presence in rate control allows the operator to perceive the surface that separates the two mappings, automatically providing a clear understanding of the robot's behavior in each instant. Conceptually the edge drift mapping described allows to map a spherical region of the local workspace in the remote workspace and to change its position by "pushing" on the region boundaries. During rate control, the operator is effectively moving the spherical working region across the environment stopping by entering in position control when actual interaction is expected. Eventually, the grasping interaction is controlled by a specific button on the haptic stylus.

2) Cable Targeting Mode: Upon the operator's request, the system can enter in *cable targeting mode*. The vision system mounted on the robot end-effector acquires an image of the environment and localizes the DLOs in it as spline functions described as vectors of points in the horizontal plane $Q_i = [Q_{ix}, Q_{iy}] \in \mathbb{R}^{nx2}$ with n the total number of points evaluating the spline. Then the closest DLO is identified as the interaction target Q and the robot motion is constrained along its main direction. In this mode edge drifting on the horizontal coordinates is disabled and the control mapping is modified to enforce the constraints: the haptic workspace is directly projected on the DLO surface so that any operator motion would result in a manipulator displacement along the object. At first, the spline vector describing the closest DLO Q^* is virtually reconstructed and centered in the haptic workspace

$$Q^* = K^*(Q) + D^*_{hr} \tag{5}$$

where D^*_{hr} is the position bias to center the cable and K^* is defined on the basis of the haptic workspace maximum radius r_{max} and the DLO maximum extension l_{max}

$$K^* = r_{max}/l_{max}. \tag{6}$$

Then in each control loop the stylus position P_h is projected on the spline toward normal directions to the spline curve

$$q^* \leftarrow \underset{q_i \in \mathcal{Q}^*}{\operatorname{argmin}}\ d(q_i, P_h) \tag{7}$$

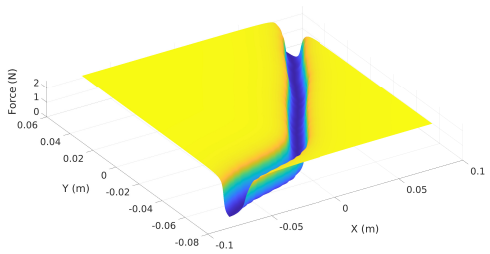

Fig. 4: Virtual fixture force feedback generated around the detected DLO shape in the haptic workspace during *cable targeting mode*.

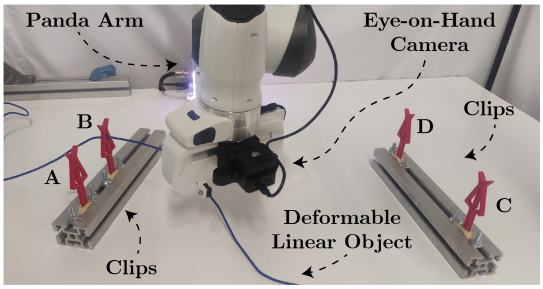

Fig. 5: Experimental setup composed of a Panda robot from Franka Emika equipped with an eye-on-hand camera.

where $d(\cdot,\cdot)$ is a generic distance function providing the spline-to-point distance. Eventually, the obtained position along the object is remapped in the remote environment by inverting eq. 5 and commanded as a reference for the robot. Along the vertical direction, the edge drifting mapping is kept active to allow a quick motion to the correct height. In order to speed up the grasping procedure the initial position bias D_{hr} is redefined closer to the horizontal plane to prepare the operator for the picking procedure. Moreover, the manipulator end-effector is naturally oriented perpendicularly to the DLO main direction at the current point, guaranteeing an effective grasp position for the gripper. In *cable targeting mode*, the operator's perception is furtherly enhanced by a virtual fixture generation through haptic feedback of the DLO shape. A potential map generating an attractive force F_{vf} toward the cable shape is generated as a function of the distance from the DLO according to an arctangent behavior

$$F_{vf} = -(\frac{1}{2} + \text{atan}(d(q^*, P_h)K_{vf})) \tag{8}$$

with K_{vf} characterizing the gradient of the force moving toward the DLO shape as presented in Fig. 4.

3) Remote Manipulator Control: The remote manipulator is controlled through an impedance control scheme directly commanding the torque reference fed to the joints. This choice allows to produce the required real-time replica of the operator motion while guaranteeing at the same time the safety of the interaction by properly imposing the impedance behavior. The dynamic model of a manipulator in the joint space can be defined as:

$$M(x)\ddot{x} + C(x,\dot{x})\dot{x} + g(x) = F_{\text{input}} + F_{ext}, \tag{9}$$

with $M(x) \in \mathbb{R}^{m\times m}$, $C(x,\dot{x}) \in \mathbb{R}^{m\times m}$ and $g(x) \in \mathbb{R}^m$ the inertia, Coriolis-Centrifugal and gravity term respectively, defined in the workspace as a function of the robot end-effector pose x and F_{ext} the vector of external forces applied by the environment and with m the dimension of the task space. The control input F_{input}, defined as:

$$F_{\text{input}} = \hat{C}(x,\dot{x}) + \hat{g}(x) + F_{impedance}, \tag{10}$$

is characterized by two different control actions: the compensation of the nonlinear dynamics expressed by the Coriolis-Centrifugal matrix and gravity term $\hat{C}(x,\dot{x}) + \hat{g}(x)$ and the definition of the desired impedance dynamic (where the impedance Inertia matrix is considered the same as the manipulator's):

$$F_{impedance} = K_p(P_r - x) - K_d\dot{x}, \tag{11}$$

where $K_p, K_d \in \mathbb{R}^{6\times6}$ are positive definite matrices imposing the desired behavior, and P_r is the reference position guided by the operator's motions on the haptic device.

IV. Experiments

The proposed teleoperation framework was evaluated through the experimental setup presented in Fig. 5. The system was mounted on an UBUNTU 20.04 operating system with an NVIDIA RTX 2080 Ti GPU running on the ROS framework. The operator was controlling a Franka Emika Panda robot through a 3DSystems Geomagic haptic device.

The visual perception of the DLO was accomplished by means of 2D RGB images acquired from an OAK-D camera by Luxonis. It is a device composed of an RGB sensor at the center and two monochrome sensors at the sides. In this work, only the RGB sensor is employed.

The control parameters chosen for the test were defined as a trade-off between control efficiency and intuitivity of motion for the human operator and are reported in Tab. I.

The experimental test was motivated by a use-case scenario of the REMODEL project, where specific cables in the environment had to be routed through specific clips to obtain a predefined configuration. Nonetheless, it can be easily compared to any scenario in which DLOs have to be manipulated and interacted with the environment. The test was performed engaging 10 healthy subjects (2 females, 8 males age: 29 $\pm$ 4 $-$ right-handed: 9 sbjs., left-handed: 1 sbj) with no prior knowledge of the setup. All tests were performed in accordance with the Declaration of Helsinki and all participants were thoroughly informed about the experimental

TABLE I: Control parameters for the experiments.

symbol	description	value
K	scale factor	1
K_f	elastic feedback gain	80
$K_p(linear)$	impedance elastic linear gain	800
$K_p(angular)$	impedance elastic angular gain	40
$K_d(linear)$	impedance damping linear gain	56.56
$K_d(angular)$	impedance damping angular gain	12.64
r_h	spherical region radius	$0.06m$
r_{max}	haptic workspace radius	$0.09m$
V_{max}	maximum robot linear velocity	$0.3m/s$

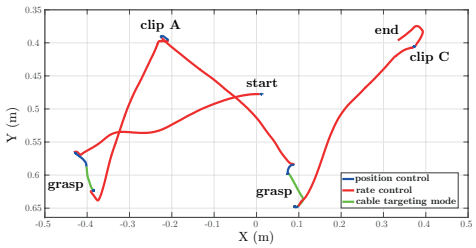

Fig. 6: Motion on the horizontal plane of the remote manipulator during a single trial. Different control modes are highlighted: position control (blue) and rate control (red) for the *free teleoperation mode*, and *cable targeting mode* (green).

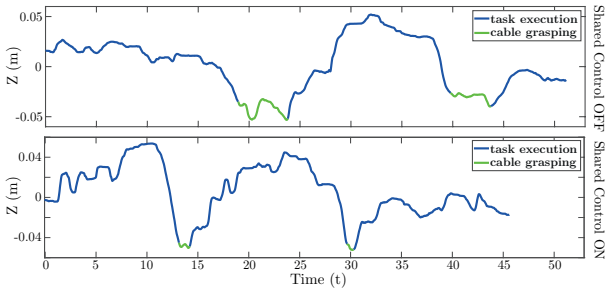

Fig. 7: Comparison between the trajectories of execution along the vertical axis of a single subject with/without the shared control framework. The grasping phase of the cable is highlighted with respect to the remaining of the task.

protocol and were asked to sign an informed consent form. The experimental protocol is described as follows. Each subject was asked to perform several manipulation tests consisting of multiple insertions of a cable in specific clips fixed in the environment as shown in Fig. 5. In each test, the operator was asked to move the robot in position to grasp a specific point along the DLO shape and perform a first insertion in clip A or B. Then, it was asked to grasp at the cable at a random point further along its shape and perform a second insertion in clip C or D. The operation was repeated three times with the *free teleoperation mode* only and three additional times exploiting also the *cable targeting mode*. In each of the three sequences with the *free teleoperation mode*, a different coupling between clips {A,B} and clips {C,D} was selected. The same couples were repeated then also with the exploitation of the *cable targeting mode*. Before the tests, each subject was given five minutes of initial training time to experiment with the system and acquire confidence. The overall task time for each sequence was measured to evaluate the effectiveness of the proposed approach. Moreover, each subject was asked to fill out a questionnaire to measure the user experience and the intuitiveness of the proposed framework.

A. Single subject results

In the following the results for a single test subject during the test involving clips A and C are reported. In Fig. 6 a complete view of the remote manipulator motion projected in the horizontal plane is presented. The spatial motion is differentiated between the different control modes: *free teleoperation* position control as a blue segment, *free teleoperation* rate control as a red segment, and *cable targeting mode* control as a green segment. The manipulator is initially placed at the center of the environment (start position) and then moved toward the cable to perform the first grasp (section on the left in the figure). The cable is dragged across the environment and inserted in the first clip (i.e. A). Eventually, the manipulator is moved toward a further section of the cable for the next grasp (section to the right in the figure) and the cable is placed in the second clip (i.e. C). From the graph, it is easy to notice that most of the motion is performed in exploiting rate control to move the spherical position control area across the environment while the position control was exploited only during high precision tasks as the clip insertions or simply traversed to move to and from the grasping operations. Eventually, the *cable targeting mode* was exploited during the precise grasp of the DLO.

From Fig. 7 it is also possible to appreciate the different performance provided by the shared control framework as highlighted in the grasping phase (green segment) with respect to the rest of the motion (blue segment). As can be clearly seen, the shared control framework produces a clear reduction in the execution time of the grasping operation, allowing the operator to mainly focus on the remaining of the task.

B. Complete test results

In the following, the complete results for the test comparing all test subjects are presented. In particular, the metric Task Completion Time (TCT) was analyzed in order to compare the performance of the subjects with and without the aid of the proposed shared control approach. Therefore, a one-way repeated measure Analysis of Variance (ANOVA) was planned to be conducted between the two data groups composed by the mean TCT over the three experimental trials carried out by each subject with the shared control switched OFF and ON, respectively, as reported in the boxplots of Fig. 8. In other words, we compared the resulting subjects' mean TCTs with and without shared control. The statistically significant difference level was set to $p < .05$. The Kolmogorov-Smirnov normality test revealed that the null hypothesis that the data groups came from a standard normal distribution was rejected at the 5% level. Therefore, as ordinary procedure in these cases, instead of the initially planned ANOVA, we performed the nonparametric Kruskal-Wallis one-way analysis, which revealed that the mean TCT resulted to be statistically significantly lower in presence of the shared control aid, $\chi^2(1) = 4.48$, $p = .03$. The positive effect of the proposed approach was therefore reflected in the TCT metrics with statistical evidence.

Moreover the results from the questionnaire are proposed in Tab. II. The proposed framework was indeed considered effective in providing further assistance and intuitiveness for the teleoperation task with respect to a standard control framework. In particular the effectiveness in simplifying the required task (PU1) and decreasing the workload for the operator (C1/C2) were highlighted.

TABLE II: User experience. Mean scores values computed over the subjects (± st. deviation): Likert scale from 1 (entirely disagree) to 7 (entirely agree.)

Outcome type		Questionnaire	Shared Control OFF	Shared Control ON
Perceived ease of use	PE1	*It was easy to teleoperate the robot manipulator for the required task.*	5.2±0.94	6.1±0.47
	PE2	*The provided teleoperation framework was easy to interpret.*	6.2±0.52	6.3±0.63
Usefulness	PU1	*I think the system provided facilitated the teleoperation task.*	4.8±1.23	6.5±0.81
Emotions	E1	*I liked to teleoperate the robotic manipulator with the proposed framework.*	6.0±0.92	6.3±0.82
Comfort	C1	*The provided system was appropriate to perform the required teleoperation task.*	5.3±1.23	6.2±0.85
	C2	*It was helpful in terms of cognitive effort to teleoperate the robot for the required goals.*	5.4±0.70	6.2±0.51

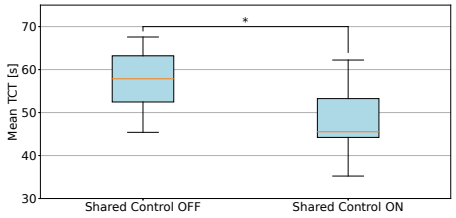

Fig. 8: Boxplot of the subjects' mean Task Completion Times (TCTs) with and without the shared control aid. The symbol "*" indicates statistically significantly difference with $p < .05$.

V. Conclusions

In this work a novel shared control framework to improve the performance and intuitiveness of DLO manipulation tasks was presented. The reconstruction of the DLO shape through the camera system provided a clear simplification of the grasping procedure, allowing the operator to focus on the remaining part of the control task. An experimental session carried out with ten healthy subjects proved the effectiveness of the proposed framework in reducing the operator's mental fatigue and in improving the overall performances. Future works will focus on the extension of the proposed framework in cluttered environments with partially occluded cable and on the improvement of the vision system to produce a complete real-time 3D detection during the operator motions.

References

[1] S. Jin, C. Wang, and M. Tomizuka, "Robust deformation model approximation for robotic cable manipulation," in *Proc. IEEE/RSJ Int. Conf. IROS*. IEEE, 2019.

[2] F. Mou, H. Ren, B. Wang, and D. Wu, "Pose estimation and robotic insertion tasks based on yolo and layout features," *Engineering Applications of Artificial Intelligence*, 2022.

[3] N. Lv, J. Liu, and Y. Jia, "Dynamic modeling and control of deformable linear objects for single-arm and dual-arm robot manipulations," *IEEE Transactions on Robotics*, 2022.

[4] J. Zhu, B. Navarro, P. Fraisse, A. Crosnier, and A. Cherubini, "Dual-arm robotic manipulation of flexible cables," in *Proc. IEEE/RSJ Int. Conf. IROS*. IEEE, 2018.

[5] Y. She, S. Wang, S. Dong, N. Sunil, A. Rodriguez, and E. Adelson, "Cable manipulation with a tactile-reactive gripper," *The International Journal of Robotics Research*, 2021.

[6] Y. Gao, Z. Chen, J. Lin, X. Li, and Y.-H. Liu, "Development of an automated system for the soldering of usb cables," *Robotics and Computer-Integrated Manufacturing*, 2023.

[7] M. Rambow, T. Schauß, M. Buss, and S. Hirche, "Autonomous manipulation of deformable objects based on teleoperated demonstrations," in *Proc. IEEE/RSJ Int. Conf. IROS*. IEEE, 2012.

[8] K. P. Cop, A. Peters, B. L. Žagar, D. Hettegger, and A. C. Knoll, "New metrics for industrial depth sensors evaluation for precise robotic applications," in *Proc. IEEE/RSJ Int. Conf. IROS*, 2021.

[9] M. Yan, Y. Zhu, N. Jin, and J. Bohg, "Self-supervised learning of state estimation for manipulating deformable linear objects," *IEEE robotics and automation letters*, 2020.

[10] A. Keipour, M. Bandari, and S. Schaal, "Deformable one-dimensional object detection for routing and manipulation," *IEEE Robotics and Automation Letters*, 2022.

[11] Y. Wang, D. McConachie, and D. Berenson, "Tracking partially-occluded deformable objects while enforcing geometric constraints," in *2021 IEEE Int. Conf. ICRA*. IEEE, 2021.

[12] D. D. Gregorio, G. Palli, and L. D. Stefano, "Let's take a walk on superpixels graphs: Deformable linear objects segmentation and model estimation," in *Asian Conference on Computer Vision*. Springer, 2018.

[13] A. Caporali, R. Zanella, D. De Gregorio, and G. Palli, "Ariadne+: Deep learning-based augmented framework for the instance segmentation of wires," *IEEE Transactions on Industrial Informatics*, 2022.

[14] A. Caporali, K. Galassi, R. Zanella, and G. Palli, "Fastdlo: Fast deformable linear objects instance segmentation," *Robotics and Automation Letters*, 2022.

[15] R. Zanella, A. Caporali, K. Tadaka, D. De Gregorio, and G. Palli, "Auto-generated wires dataset for semantic segmentation with domain-independence," in *Proc. of the ICCCR*, 2021.

[16] A. Caporali, M. Pantano, L. Janisch, D. Regulin, G. Palli, and D. Lee, "A weakly supervised semi-automatic image labeling approach for deformable linear objects," *IEEE Robotics and Automation Letters*, 2023.

[17] F. Conti and O. Khatib, "Spanning large workspaces using small haptic devices," in *First Joint Eurohaptics Conference and Symposium on Haptic Interfaces for Virtual Environment and Teleoperator Systems. World Haptics Conference*. IEEE, 2005.

[18] Z. Jiang, F. Ni, D. Yang, C. Li, F. Yang, and H. Liu, "A hybrid mapping method with position and stiffness for manipulator teleoperation," *Applied Sciences*, 2019.

[19] A. Pepe, D. Chiaravalli, and C. Melchiorri, "A hybrid teleoperation control scheme for a single-arm mobile manipulator with omnidirectional wheels," in *Proc. IEEE/RSJ Int. Conf. IROS*. IEEE, 2016.

[20] S. Gou, J. Zhou, H. Zhang, M. Liu, S. Yang, and X. Zhang, "Workspace mapping method based on edge drifting for the teleoperation system," in *Journal of Physics: Conference Series*. IOP Publishing, 2022.

[21] D. A. Abbink, M. Mulder, and E. R. Boer, "Haptic shared control: smoothly shifting control authority?" *Cogn Technol Work*, 2012.

[22] T.-C. Lin, A. U. Krishnan, and Z. Li, "Shared autonomous interface for reducing physical effort in robot teleoperation via human motion mapping," in *Proc. Int. Conf. ICRA*. IEEE, 2020.

[23] M. Laghi, L. Raiano, F. Amadio, F. Rollo, A. Zunino, and A. Ajoudani, "A target-guided telemanipulation architecture for assisted grasping," *IEEE Robotics and Automation Letters*, 2022.

[24] D. Ding, B. Styler, C.-S. Chung, and A. Houriet, "Development of a vision-guided shared-control system for assistive robotic manipulators," *Sensors*, 2022.

[25] A. Gottardi, S. Tortora, E. Tosello, and E. Menegatti, "Shared control in robot teleoperation with improved potential fields," *IEEE Transactions on Human-Machine Systems*, 2022.

[26] V. Pruks and J.-H. Ryu, "Method for generating real-time interactive virtual fixture for shared teleoperation in unknown environments," *The International Journal of Robotics Research*, 2022.